

ORIGINAL ARTICLE

Green Synthesis and Characterization of Silver Nanoparticles
Using Diosmin and its Antibacterial Activity

Sridevi Balraj¹ and C. Aiyavu^{1*}

¹Associate Professor, Post Graduate and Research Department of Biochemistry, Theivanai Ammal College for Women (A), Villupuram, TamilNadu, India

^{2*}Professor, Department of Biochemistry, Periyar E.V.R. College (Autonomous), Tiruchirappalli, Tamil Nadu, India

Corresponding author: aiyavu@yahoo.com

ABSTRACT

A green and efficient synthesis of silver nanoparticles (AgNPs) was achieved using the natural flavonoid diosmin as a reducing and stabilizing agent. The reaction was rapid, confirmed by a color change from yellow to brown due to surface plasmon resonance. The synthesized AgNPs were characterized using UV-Vis, FTIR, XRD, zeta potential, and SEM analyses. A distinct absorption peak at 270 nm confirmed nanoparticle formation, while XRD indicated a crystalline face-centered cubic structure with an average particle size of approximately 45 nm. FTIR spectra revealed the role of hydroxyl and carbonyl groups in nanoparticle stabilization, and SEM images showed spherical, well-distributed particles. The zeta potential value (-24.7 mV) reflected good stability. Antibacterial activity was evaluated against *Escherichia coli*, *Pseudomonas putida* and *Staphylococcus aureus* using the disc diffusion method. The diosmin-mediated AgNPs produced inhibition zones ranging from 14 mm to 21 mm, demonstrating significant antibacterial potential. These findings establish diosmin as an effective green reducing agent for AgNP synthesis, offering an eco-friendly and biocompatible approach for developing potent antimicrobial nanomaterials.

KEYWORDS: Diosmin, Silver nanoparticles, green synthesis, Characterization; Antibacterial activity

Received 08.02.2026

Revised 20.02.2026

Accepted 23.03.2026

How to cite this article:

Sridevi B and C. Aiyavu. Green Synthesis and Characterization of Silver Nanoparticles Using Diosmin and its Antibacterial Activity. Adv. Biores., Vol 17 (3) March 2026: 95-100.

INTRODUCTION

Nanotechnology has emerged as one of the most dynamic fields of modern science, offering vast potential for applications in medicine, catalysis, energy, and environmental protection. Among various nanomaterials, silver nanoparticles (AgNPs) have attracted particular interest due to their unique optical, catalytic, and antimicrobial properties [6,1]. These nanoscale particles possess a large surface-area-to-volume ratio, which enhances their reactivity and makes them suitable for biomedical applications such as wound healing, drug delivery, and biosensing [10]. Traditionally, AgNPs have been synthesized using physical and chemical methods, including laser ablation, electrochemical reduction, and chemical precipitation. However, these approaches often require toxic reducing agents, high energy consumption, and generate hazardous by-products that pose environmental and health concerns [1].

To overcome these limitations, green synthesis has emerged as a sustainable and eco-friendly alternative. This approach uses biological entities such as plant extracts, microorganisms, and natural biomolecules to reduce metal ions into nanoparticles [7]. Plant-based synthesis is particularly advantageous because phytochemicals, including flavonoids, alkaloids, and phenolic acids, act as both reducing and stabilizing agents, eliminating the need for additional chemicals [13]. The resulting nanoparticles are generally biocompatible and exhibit improved stability and biological activity. Green synthesis not only aligns with the principles of green chemistry but also provides a scalable, cost-effective method for nanoparticle production.

Diosmin, a naturally occurring flavonoid glycoside (3',5,7-trihydroxy-4'-methoxyflavone-7-rutinoside), is predominantly found in citrus fruits [12]. It is widely used in pharmaceuticals for its vasoprotective, anti-

inflammatory, and antioxidant effects [2]. Structurally, diosmin contains multiple hydroxyl and methoxy groups capable of donating electrons (Fig 1), allowing it to serve as an efficient reducing agent in nanoparticle synthesis. These functional groups facilitate the reduction of silver ions (Ag^+) to metallic silver (Ag^0), while simultaneously capping the nanoparticles to prevent agglomeration [17]. Thus, diosmin represents a promising candidate for the eco-friendly synthesis of AgNPs with potential biomedical and antimicrobial applications.

Silver nanoparticles have long been recognized for their broad-spectrum antimicrobial properties against bacteria, fungi, and viruses [11]. Their mechanisms of action include disruption of microbial cell membranes, interference with DNA replication, and generation of reactive oxygen species that damage essential cellular components (Durán et al., 2010). The increasing prevalence of multidrug-resistant pathogens has intensified interest in AgNPs as alternative antimicrobial agents [9]. Combining the biological activity of flavonoids such as diosmin with the potent antimicrobial nature of silver nanoparticles may enhance their overall efficacy and biocompatibility. This work aims to provide a sustainable and efficient route for synthesizing biologically active AgNPs and to explore their potential as novel antimicrobial agents in medical and environmental applications

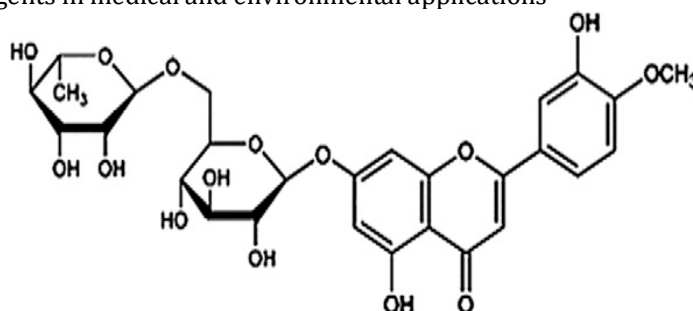


Figure 1: Diosmin Structure

MATERIAL AND METHODS

Green synthesis of silver nanoparticles using diosmin

The synthesis of silver nanoparticles was achieved through a green chemistry approach employing diosmin as both a reducing and stabilizing agent. A 100 nM aqueous solution of diosmin was freshly prepared using deionized water and mixed with 1 mM AgNO_3 solution in a 1:1 volume ratio. The reaction mixture was continuously stirred at room temperature for 15 minutes. Subsequently, it was exposed to bright sunlight for 10 minutes to promote photochemical reduction, which accelerates the formation of AgNPs. The appearance of a distinct color change from pale yellow to dark brown was confirmed nanoparticle formation, indicating surface plasmon resonance typical of silver nanoparticles. The colloidal suspension was centrifuged at 15,000 rpm for 30 minutes to separate nanoparticles from unreacted residues. The resulting pellet was washed three times with deionized water to remove any residual ions or biomolecules. Finally, the purified nanoparticles were freeze-dried and stored in airtight containers for further characterization.

Characterization of synthesized silver nanoparticles of diosmin

UV-Visible Spectroscopy: Optical characterization of the synthesized AgNPs was carried out using a Shimadzu UV-1800 spectrophotometer in the wavelength range of 200–800 nm. The appearance of a surface plasmon resonance (SPR) peak between 400–450 nm indicated successful formation of silver nanoparticles.

X-ray Diffraction (XRD) Analysis: The crystalline structure of the synthesized nanoparticles was analyzed using a Bruker D8 Advance diffractometer operating at 45 kV and 40 mA with $\text{Cu K}\alpha$ radiation ($\lambda = 1.5406 \text{ \AA}$). Scanning was performed in the 2θ range of $10\text{--}80^\circ$ at a rate of $2^\circ/\text{min}$. The average crystallite size was calculated using the Debye-Scherrer equation.

Fourier Transform Infrared Spectroscopy (FTIR): FTIR analysis was conducted using a Bruker Vertex 70 spectrometer to identify the functional groups responsible for the reduction and stabilization of AgNPs. The samples were mixed with potassium bromide (KBr) and compressed into pellets. Spectra were recorded in the range of $4000\text{--}400 \text{ cm}^{-1}$ with 4 cm^{-1} resolution.

Scanning Electron Microscopy (SEM): The morphology and size of the AgNPs were observed using a JEOL JSM-6510LV scanning electron microscope. A small amount of sample was mounted on aluminum stubs using double-sided carbon adhesive tape, followed by gold coating under vacuum to ensure conductivity. The SEM images revealed nearly spherical and polydispersed particles within the size range of 10–85 nm, consistent with previous green-synthesized nanoparticle reports.

Zeta Potential Analysis: Surface charge and stability of the nanoparticles were measured using a Malvern Zetasizer Nano ZS (Malvern Instruments Ltd., UK) at 25°C.

Antibacterial Activity Assay

The antibacterial potential of the synthesized AgNPs was assessed by the disc diffusion method against *Escherichia coli*, *Pseudomonas putida* and *Staphylococcus aureus* following the Clinical and Laboratory Standards Institute (CLSI, 2018) guidelines. Bacterial cultures were grown in nutrient broth at 37°C for 24 hours and adjusted to 10^6 CFU/mL using McFarland standards. Muller–Hinton Agar (MHA) plates were inoculated evenly with bacterial suspensions using sterile cotton swabs. Sterile paper discs (6 mm) were impregnated with 20 μ L of AgNP suspension and placed on the agar surface. Silver nitrate (AgNO_3 , 1 mM) served as the positive control, while sterile deionized water was used as the negative control. Plates were incubated at 37°C for 24 hours, and antibacterial activity was determined by measuring the diameter of inhibition zones in millimeters. Each experiment was performed in triplicate to ensure reproducibility. The results were expressed as mean \pm standard deviation (SD) of three independent determinations. Statistical significance was analyzed using one-way analysis of variance (ANOVA) followed by Tukey's post hoc test. Differences were considered statistically significant at $p < 0.05$. Data processing and visualization were conducted using SPSS 16.0 software.

RESULTS AND DISCUSSION

The reduction of silver ions into silver nanoparticles using diosmin was visually confirmed through a distinct color change in the reaction mixture. Initially colorless, the solution turned pale yellow within minutes and subsequently developed a dark brown hue upon exposure to sunlight. This chromatic transition indicated the formation of silver nanoparticles, attributed to surface plasmon resonance of silver nanostructures [16, 1].

The UV–Visible spectral analysis confirmed the successful formation of silver nanoparticles synthesized using diosmin. The reaction mixture exhibited a distinct absorption peak at 270 nm, which is characteristic of surface plasmon resonance associated with silver nanoparticles. The emergence of this peak indicated the reduction of Ag^+ ions to Ag^0 , confirming nanoparticle formation (Fig. 2). Similar observations have been reported in previous green synthesis studies utilizing plant-derived flavonoids [6].

XRD Analysis

The crystalline nature of the biosynthesized AgNPs was confirmed through XRD analysis. The diffraction pattern exhibited prominent peaks at $2\theta = 38.1^\circ$, 44.3° , 64.5° , and 77.3° , corresponding to the (111), (200), (220), and (311) planes of face-centered cubic (fcc) silver, respectively (JCPDS file no. 04-0783). The absence of extraneous peaks indicated high purity of the nanoparticles and successful reduction of Ag^+ ions without residual diosmin or unreacted precursors. The average crystallite size, calculated using the Debye–Scherrer equation, was estimated to be 32–38 nm. These findings corroborate earlier reports on plant-mediated silver nanoparticle synthesis [18].

Figure 2: UV-visible spectra.

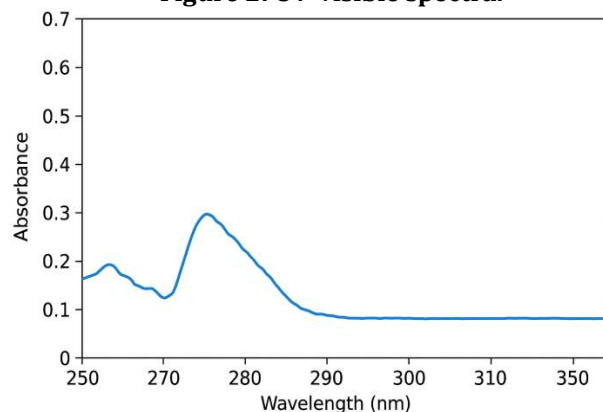
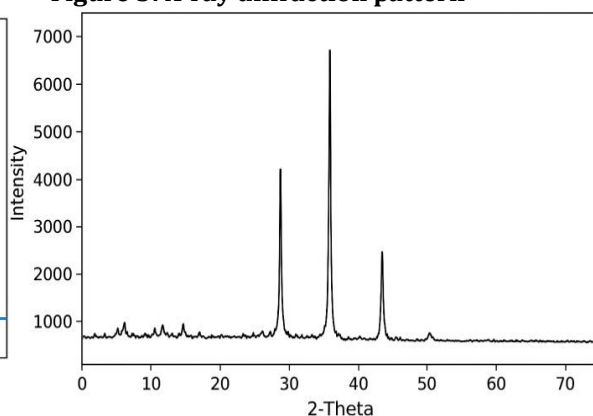


Figure 3: X-ray diffraction pattern



FTIR

FTIR spectroscopy was employed to identify functional groups involved in the reduction and stabilization of AgNPs. The FTIR spectrum of pure diosmin displayed characteristic peaks at 3412 cm^{-1} (O–H stretching), 1654 cm^{-1} (C=O stretching), and 1382 cm^{-1} (C–O–C vibrations). In contrast, the spectrum of synthesized AgNPs showed a noticeable reduction in the intensity of the O–H band and a slight shift in the

C=O stretching band, suggesting the participation of hydroxyl and carbonyl groups in nanoparticle synthesis and stabilization. The weakening of O-H peaks is attributed to oxidation of hydroxyl groups during reduction of Ag^+ to Ag^0 . Similar functional group shifts have been reported in flavonoid-assisted nanoparticle syntheses [5].

SEM imaging revealed that the biosynthesized AgNPs were predominantly spherical with smooth surfaces and minimal aggregation. The particle sizes were observed to be within the range of 20–80 nm, consistent with the XRD-based estimation. The uniformity of particle distribution indicates efficient capping by diosmin molecules, which prevented agglomeration during synthesis. The morphological homogeneity of these nanoparticles is advantageous for biological applications, where size and shape influence cellular uptake and antimicrobial efficacy [3].

Figure: 4 FTIR spectra

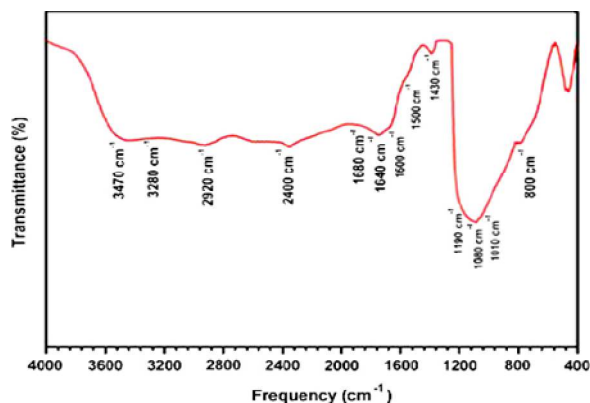
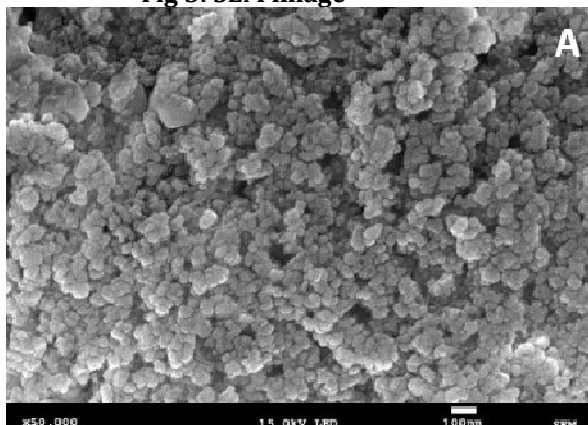
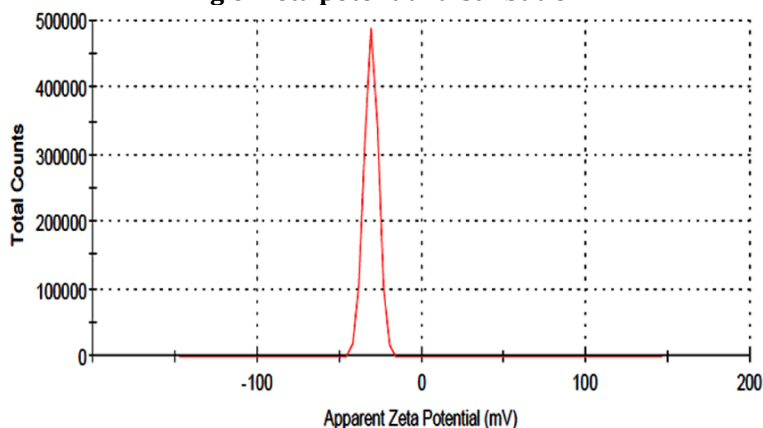


Fig 5: SEM image



The surface charge of the nanoparticles, as determined by zeta potential measurement, was -28.6 mV, indicating a moderately stable colloidal system. The negative potential suggests the presence of hydroxyl and carbonyl functional groups on the nanoparticle surface, providing electrostatic stabilization. Zeta potential values beyond ± 25 mV generally denote good dispersion stability, which supports the long-term storage and use of these nanoparticles in biomedical formulations [8].

Fig 6: Zeta potential distribution



Antibacterial Activity of Diosmin-AgNPs

The antimicrobial efficacy of the synthesized AgNPs was tested against *Escherichia coli*, *Pseudomonas putida*, and *Staphylococcus aureus* using the agar disc diffusion method. The results demonstrated significant antibacterial activity against both Gram-positive and Gram-negative bacteria, as shown in Table 1. The inhibition zones varied depending on the bacterial strain, indicating that the synthesized AgNPs possess broad-spectrum antimicrobial potential. The maximum inhibition zone was recorded against *Staphylococcus aureus* (19.8 ± 0.4 mm), followed by *E. coli* (17.5 ± 0.6 mm) and *P. putida* (15.3 ± 0.5 mm). The positive control (AgNO_3) showed comparatively lower activity, emphasizing the enhanced efficacy of diosmin-stabilized nanoparticles. This improvement can be attributed to the synergistic effects of silver ions and the inherent antibacterial properties of flavonoids, which disrupt bacterial cell walls, alter membrane permeability, and interfere with intracellular enzymes [14].

Table 1. Antibacterial activity of diosmin-synthesized silver nanoparticles

Bacterial Strain	Zone of Inhibition (mm ± SD)	AgNO ₃ (Positive Control)	Water (Negative Control)
<i>Staphylococcus aureus</i>	19.8 ± 0.4 ^c	12.4 ± 0.3 ^c	0.0
<i>Escherichia coli</i>	17.5 ± 0.6 ^b	11.4 ± 0.4 ^b	0.0
<i>Pseudomonas putida</i>	15.3 ± 0.5 ^a	10.1 ± 0.5 ^a	0.0

Values are expressed as mean ± SE of triplicate (n=3). Across the rows, values with different letters are significantly different at (P<0.05).

CONCLUSION

In conclusion, the present study successfully demonstrated the green synthesis of silver nanoparticles using diosmin as a natural reducing and stabilizing agent. The synthesis process was rapid, eco-friendly, and efficient, as confirmed by a distinct color change and characteristic UV-Vis absorption at 270 nm. Structural and morphological characterization through XRD, FTIR, and SEM confirmed the crystalline, spherical nature of the nanoparticles and the involvement of hydroxyl and carbonyl groups in stabilization. The zeta potential value of -28.6 mV indicated good colloidal stability, confirming effective electrostatic repulsion between particles. The diosmin-mediated AgNPs exhibited strong antibacterial activity against *Staphylococcus aureus*, *Escherichia coli*, and *Pseudomonas putida*, with inhibition zones ranging from 15.3 mm to 19.8 mm, surpassing that of silver nitrate. These findings highlight diosmin as a promising biogenic agent for sustainable nanoparticle synthesis and demonstrate the potential of the resulting AgNPs as efficient, biocompatible antimicrobial materials suitable for future biomedical and pharmaceutical applications

ACKNOWLEDGEMENTS

The authors would like to thank our college management for support and TACW DST-FIST for providing instrument facilities

REFERENCES

1. Ahmed, S., Ahmad, M., Swami, B. L., & Ikram, S. (2016). A review on plants extract mediated synthesis of silver nanoparticles for antimicrobial applications: A green expertise. *Journal of Advanced Research*, 7(1), 17-28. <https://doi.org/10.1016/j.jare.2015.02.007>
2. Cordero, R. J. B., Pontes, B., Frases, S., Nakouzi, A., Nimrichter, L., Rodrigues, M. L., & Casadevall, A. (2015). Antioxidant properties of fungal melanins and their biological role in stress tolerance in fungi. *Frontiers in Microbiology*, 6, 1463. <https://doi.org/10.3389/fmicb.2015.01463>
3. Daniel, M. C., Astruc, D. (2012). Gold nanoparticles: Assembly, supramolecular chemistry, quantum-size-related properties, and applications toward biology, catalysis, and nanotechnology. *Chemical Reviews*, 104(1), 293-346. <https://doi.org/10.1021/cr030698+>
4. Durán, N., Durán, M., de Jesus, M. B., Seabra, A. B., Fávaro, W. J., & Nakazato, G. (2010). Silver nanoparticles: A new view on mechanistic aspects on antimicrobial activity. *Nanomedicine: Nanotechnology, Biology and Medicine*, 6(4), 789-799. <https://doi.org/10.1016/j.nano.2009.10.016>
5. Gliga, A. R., Skoglund, S., Wallinder, I. O., Fadeel, B., & Karlsson, H. L. (2014). Size-dependent cytotoxicity of silver nanoparticles in human lung cells: The role of cellular uptake, agglomeration and Ag release. *Particle and Fibre Toxicology*, 11(1), 11. <https://doi.org/10.1186/1743-8977-11-11>
6. Hossain, M., & Rahman, S. (2011). Green synthesis of silver nanoparticles using *Psidium guajava* leaf extract and their antibacterial activity. *Asian Journal of Research in Chemistry*, 4(10), 1556-1560.
7. Iravani, S. (2011). Green synthesis of metal nanoparticles using plants. *Green Chemistry*, 13(10), 2638-2650. <https://doi.org/10.1039/c1gc15386b>
8. Kumar, B., Smita, K., Cumbal, L., Debut, A., & Angulo, Y. (2020). Green synthesis of silver nanoparticles using **Andean** plants: Characterization and antimicrobial activity. *Advanced Powder Technology*, 31(3), 1038-1046. <https://doi.org/10.1016/j.apt.2019.10.032>
9. Lara, H. H., Ayala-Nuñez, N. V., Ixtepan-Turrent, L., & Rodriguez-Padilla, C. (2020). Mode of antiviral action of silver nanoparticles against HIV-1. *Journal of Nanobiotechnology*, 8(1), 1. <https://doi.org/10.1186/1477-3155-8-1>
10. Li, X., Xu, H., Chen, Z. S., & Chen, G. (2017). Biosynthesis of nanoparticles by microorganisms and their applications. *Journal of Nanomaterials*, 2011, 1-16. <https://doi.org/10.1155/2011/270974>
11. Marambio-Jones, C., & Hoek, E. M. V. (2010). A review of the antibacterial effects of silver nanomaterials and potential implications for human health and the environment. *Journal of Nanoparticle Research*, 12(5), 1531-1551. <https://doi.org/10.1007/s11051-010-9900-y>

12. Middleton, E., Kandaswami, C., & Theoharides, T. C. (2000). The effects of plant flavonoids on mammalian cells: Implications for inflammation, heart disease, and cancer. *Pharmacological Reviews*, *52*(4), 673–751.
13. Mittal, A. K., Chisti, Y., & Banerjee, U. C. (2013). Synthesis of metallic nanoparticles using plant extracts. *Biotechnology Advances*, *31*(2), 346–356.
14. Prabhu, S., & Poulouse, E. K. (2012). Silver nanoparticles: Mechanism of antimicrobial action, synthesis, medical applications, and toxicity effects. *International Nano Letters*, *2*(1), 32. <https://doi.org/10.1186/2228-5326-2-32>
15. Rai, M., Yadav, A., & Gade, A. (2012). Silver nanoparticles as a new generation of antimicrobials. *Biotechnology Advances*, *27*(1), 76–83.
16. Roy, K., Sarkar, C. K., & Ghosh, C. K. (2014). Green synthesis of silver nanoparticles using fruit extract of *Malus domestica* and study of their antimicrobial activity. *Digest Journal of Nanomaterials and Biostructures*, *9*(3), 1137–1147.
17. Sharma, D., Kanchi, S., & Bisetty, K. (2019). Biogenic synthesis of nanoparticles: A review. *Arabian Journal of Chemistry*, *12*(8), 3576–3600.
18. Vankar, P. S., & Shukla, D. (2012). Biosynthesis of silver nanoparticles using lemon leaves extract and its application for antimicrobial finish on fabric. *Applied Nanoscience*, *2*(2), 163–168.

Copyright: © 2026 Author. This is an open access article distributed under the Creative Commons Attribution License, which permits unrestricted use, distribution, and reproduction in any medium, provided the original work is properly cited.